MANUFACTURING OF A VARIABLE CHORD EXTENSION CONCEPT FOR HELICOPTER ROTOR BLADES WITH A FLEXIBLE EPDM SKIN

Steffen Kalow [1] , Johannes Riemenschneider [1], Christoph Balzarek [1], Torsten Mendrock [1]

[1] Institute of Composite Structures and Adaptive Systems, German Aerospace Center (DLR),
Lilienthalplatz 7, 38108 Braunschweig, Germany,
steffen.kalow@dlr.de, johannes.riemenschneider@dlr.de, torsten.mendrock@dlr.de

Abstract

In the SABRE project a new morphing concept, the so-called linear variable chord extension, has been developed. Here, the blade chord length in the root area is changed with the help of an elastic skin to adapt it to the respective flight condition. This paper focuses on the manufacturing process of the technology demonstrator and give a detailed overview about the advantages and disadvantages of handling with EPDM material. This also addresses the challenge of reinforcing the EPDM with CFRP fibers.

Keywords: manufacturing, EPDM, morphing, rotor, helicopter, trailing edge, chord extension, SABRE

1. INTRODUCTION

Since helicopter rotors have different demands from different flight stats, the final design is always a compromise between flight stats such as hover and fast forward flight. Two of the design parameters are twist and chord length. From rotor dynamic calculations it is known, that longer chord length at the blade root and increased pre-twist [1] would increase the performance in hover, whereas shorter chord and less twist is beneficial for fast forward flight. Some concepts have been shown in literature, that mainly focus on a uniform extension of the blade chord at a particular region of a blade [1][3][4]. Within [5] a performance calculation for blades with different blade shapes is given to motivate the design of a morphing rotor blade that can change the chord length in the root region. Based on this assumption, a structural concept for such a chord morphing with variable blade chord length in the blade root area was developed [6],which increases the chord linearly towards the blade root starting at a pivot point. The structural implementation of the technology into a demonstrator as well as the testing and validation was presented for both, under centrifugal forces in the DLR whirl tower and also in the wind tunnel of the University of Bristol. The simulated effects of such a technology and the advantages and disadvantages for the respective flight condition are shown in [7]. First test results of the system in whirl tower condition and also wind tunnel configuration can be found in [8].

The paper presenting here focuses on the manufacturing processes of the technology demonstrator and covers both the complex fabrication of the flexible outer skin made of EPDM, as well as the interaction of the different material components of the demonstrator in general.

2. CHORD EXTENSION CONCEPT

The final design of chord extension technology demonstrator was developed in [5] and is shown in Figure 1. As the reference rotor blade is the well-documented Bo105, the structural design is shown for the NACA 23012 profile at a chord length of 270 mm. Depending on the test facilities, the demonstrator is 1257mm long and a length of 990mm for the aerodynamic area.

The basis of the demonstrator is the hybrid spar, consisting of an aluminum component with glass fiber reinforced polymer (GFRP) strips bonded to the spar for improved bonding of the EPDM. The weight-saving pocket is covered by a dedicated lightweight lid. Nine GFRP webs and a CFRP trailing edge are attached to the spar with pins. These elements form the supporting structure for the two EPDM skins on the top and bottom of the model.

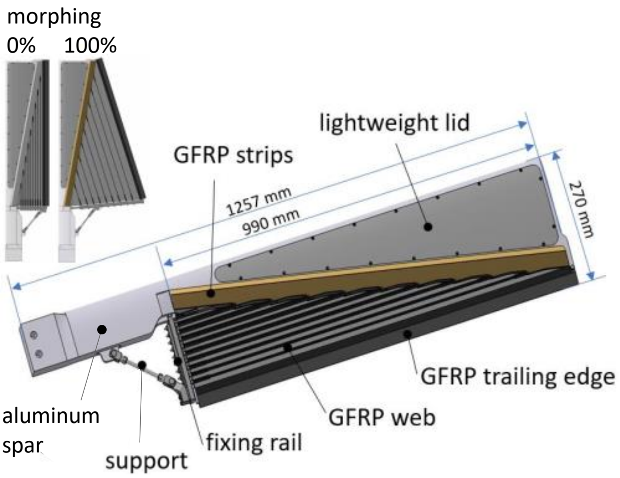

Figure 1: Principal concept and components of chord extension demonstrator

The EPDM skins are manufactured of type SAA9509-85 material from Gummiwerk KRAIBURG GmbH & Co KG (Waldkraiburg, Germany), which is part of the KRAIBON® family of materials. The material was chosen due to its low Shore hardness and its high allowable strains. Moreover, it allows for a strong bonding with thermoset materials, which is the key for the material selection.

The elastic EPDM skins allow the chord length to be extended by 100% at the root area, thus increasing the surface area of the blade profile. For this first demonstrator, the different actuation states are realized by fixing the webs and the trailing edge to a dedicated rail. For this purpose, they are screwed to a fixing rail. In order to be able to represent discrete conditions, several fixing rails have been manufactured for this testing campaign. To dissipate forces that occur in longitudinal direction of the blade, an additional support is provided between the fixing rail and the spar.

For manufacturing simplicity, the non-morphing parts of the spar, including the bolt attachment, are milled from aluminum. To reduce the weight of the demonstrator, a large pocket is included and covered with a lid. Since the attachment of the elastic skin to the aluminum is not possible, an auxiliary spar made from GFRP is attached (brown part in Figure 1), which allows for bonding of the EPDM skin. Towards the trailing edge, the individual GFRP webs are positioned by tools with complex geometry, which have to be removed after vulcanization. As a further special feature, the webs are held at the radially innermost position by an articulated guide rail, which covers the entire morphing length. An additional stiffener between the guide rail and the main spar compensates the in-plane and out-of-plane forces. The design of the individual components is primarily based on a static-mechanical FE calculation, in which the model is rotated around a virtual pivot point at a speed of 600 RPM. Additionally, aerodynamic pressure loads are applied to the model, which are based on the hover decay with maximum load. These pressure distributions are given in detail in [6].

3. FLEXIBLE EPDM SKIN

Handling with EPDM is in no way trivial when producing thin flexible skins with uniform thickness distribution and without major pore entrapment. The final manufacturing of the skins was performed with a lab calender GK300L of SAUERESSIG®. This is a teflon coated double roller system with a pull-through unit. The rolls with a diameter of 200mm and width of 300mm can be heated up to 200°C and generate a contact pressure of up to 240bar.

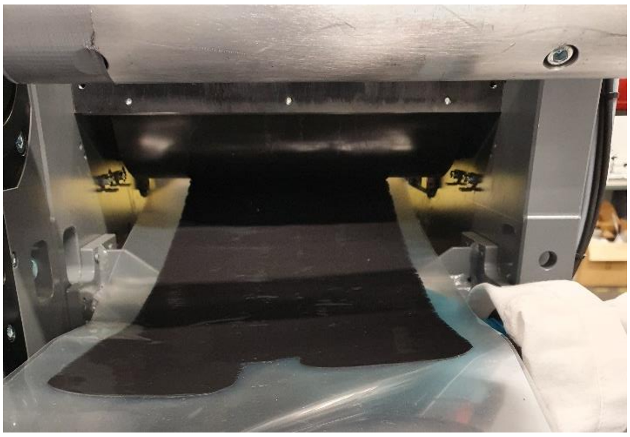

Figure 2: Output of the calender with finished EPDM skin

Numerous tests were carried out for the final manufacturing to find the correct process parameters. In this process, the EPDM is pressed through two co-rotating rolls and placed on a carrier film (Figure 2).

The release film is HOSTAPHAN® on PE-basis with 75µm thickness. The rollers move synchronously at 0.5mm/s and have a spacing of 800µm. The temperature of the rollers was 70°C. The skins of the technology demonstrator each consist of two individual EPDM layers, which are rolled on top of each other in a second step to a total thickness of approximately 1.6 mm.

During skin production, different configurations were tested for both roll temperature and roll spacing and speed. The raw material is pressed step by step by reducing the distance between rollers. If the rollers were unheated the pull-in was hardly possible, because the EPDM was too stiff for direct rolling to nominal thickness. With a temperature of 70°C the EPDM became more flexible. In some cases, this resulted in warping and a bead formation in front of calender nip (Figure 3). In order to be able to produce a homogeneous layer from this again, it was necessary to reroll several times and at the same time to observe the continuous material flow and the correct infeed of the carrier film.

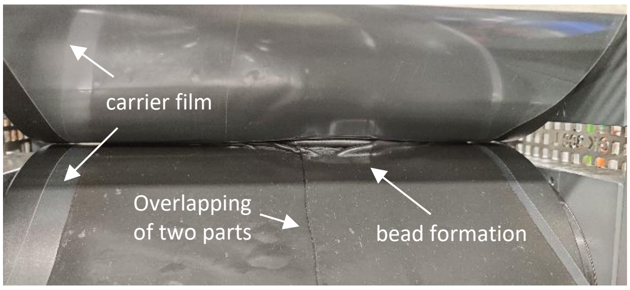

Figure 3: Bead formation in front of calender nip

At the beginning, the EPDM must be forced into the gap between the rolls by pulling on the HOSTAPHAN film. Afterwards the material is automatically pulled through by frictional forces. Several individual pieces are pressed together to form a whole skin. This results in final skins of 1000mm length and 240mm width. The overlap of two individual parts should be at least 1-2cm. When compressing two parts together, it is important not to create too many pores warpages (Figure 4). Small pores or material unevenness can be smoothed out in the final vulcanization process of the EPDM by the flowability at temperature and pressure. Anything else leads to a high risk of poorer surface quality.

It has also been shown that the roller speed is very important for rolling the EPDM including the carrier film, because if the roller speed is too fast, small distortions occur, which lead to kinks in the carrier film. These also transfer to the material, which would result in a wavy skin (Figure 5).

Figure 4: EPDM with pore (left) and material warpage (right)

Figure 5: EPDM skin with kinks in the carrier film

4. REINFORCED EPDM SKIN

In order to extend the profile in chord direction up to 100%, the skin must be very flexible. However, it should still be able to hold the profile contour in the areas between the individual GFRP webs. For this purpose, it was investigated whether the skin can be stiffened by implementing CFRP fibers as a sandwich configuration between the two individual EPDM layers in radial blade direction. There is a wide choice of fiber materials and so different types of fibers and variants of the implementation have been tried out.

First, the use of single fiber strands was investigated. Here, fiber bundles of different numbers of individual fibers were placed by hand on one side of the EPDM layer and fixed to the carrier plate (Figure 6). At the same time, the influence of the distance between the fiber strands was also investigated. In this example, the distance between the fiber bundles is 5 mm on the left and about 1 mm on the right side. Subsequently, the second EPDM layer was carefully placed on top and the sandwich structure including the carrier plate was packed in a vacuum setup. Numerous test specimens were produced in this way.

Figure 6: Implementing single CFRP fibers strands with different distances in the EPDM skin

In addition to the implementation of different single fiber strands with different fiber distances, the insertion of fiber tapes as well as a fiber blanket was also investigated (Figure 7). Analogous to the orientation of the fibers, tapes and fiber blankets were also used here, whose fibers also lie unidirectionally in the radial direction of the blade. To ensure that the fibers retain their orientation and the blanket is manageable, warp threads were used in the manufacture of the blanket.

Figure 7: Manufacturing EPDM test specimen with CFRP fiber blanket

Since these could possibly influence the properties of the stiffened EPDM skin, various test specimens were also produced here. On the one hand the original manufacturer product with warp threads were used, on the other hand they were removed mechanically or burned down with heat. In the case of burning the warp threads, the sizing of the CFRP fibers may also be burned. The testing of the specimens will show whether this has a significant effect on the bonding of the fibers with the EPDM.

As well as the skins of the final assembled technology demonstrator, the manufactured EDPM specimens were vulcanized in an autoclave at a temperature of 130°C and a pressure of 2.7bar for 120min (Figure 8).

Figure 8: Vulcanization of the EPDM specimens in autoclave

After curing, all test specimens were examined with regard to both the surface condition and the incorporation of the fibers into the EPDM. It can be summarized that almost all test specimens had a good smooth surface without a tensile load. Subsequently, all test specimens were subjected to a load in a very simple test setup, as would occur in the technology demonstrator if the skin in the root area were stretched by up to 100%. For this purpose, one side was firmly clamped and the other side was pulled transversely to the fiber under various types of load. Here, a differently pronounced unevenness in the skin surface became apparent very quickly in almost all test specimens (Figure 9).

Figure 9: Tensile test of single CFRP fibers strands with different distances in the EPDM skin (left: 1mm, right: 5mm)

Of course, this depends on the direction of the load and this simple test does not produce any scientifically reliable data. However, it does show that the implementation of single fiber strands to supposedly increase the contour fidelity of the skin in the chord morphed state is accompanied by a waviness and roughness of the skin. It can be seen that the smaller the distance between the fiber strands, the rougher the skin, which is presumably due to irregularities in the very complex individual deposition of the fibers.

It looks slightly better if 15 mm wide fiber tapes are used instead of single fiber strands (Figure 10). The distortions and unevenness are much smaller, but still noticeable and visible. The tapes simplify the manufacturing process enormously, which is also reflected in the result. However, it can already be seen that at the ends of the specimen the bonding of the fibers into the EPDM sandwich did not work as well as before with the single fiber strands. Since the EPDM material is highly viscous, the fibers are not impregnated. In the case of the single fiber strands, these were at least enclosed by the EPDM and were thus able to obtain a fairly good bond. In the case of putting tapes at each other, this is noticeably less satisfactory.

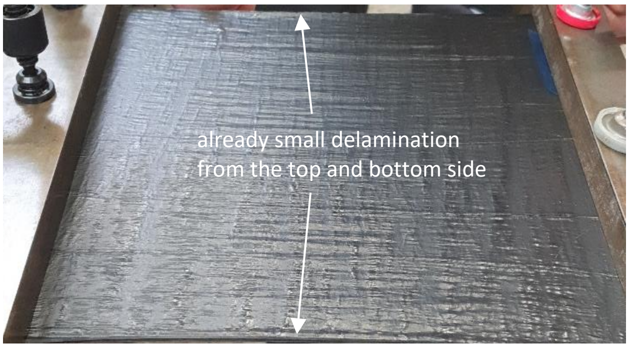

Figure 10: Tensile test of CFRP fibers tapes in the EPDM skin

This can be seen even more clearly in the test specimens with the fiber blanket. This has by far the best surface quality, even under tensile load. However, even here the skin is not really smooth, as it would be without fiber embedding. Furthermore, a clear opening between the upper and lower EPDM layer is already visible after a minimal load application (Figure 11). By pulling on both layers, the skin can be completely peeled off, which is due to the fact that no EPDM has infiltrated the dense fiber blanket and the fibers are therefore dry between the two EPDM layers. A comparison of the fiber blanket with warp threads also shows that by pulling the skin, the warp threads tear apart and the skin is then irreversibly deformed. No difference was found between mechanical or thermal removal of the warp threads. As already mentioned, the degree of impregnation and the durability of the overall composite was insufficient for this.

Figure 11: CFRP fibers blanket in the EPDM skin before tensile test

Unfortunately, due to the advanced project schedule, it was not possible to carry out further tests. Therefore, the knowledge gained from the tests to stiffen the EPDM skin in order to reduce possible deformation under high centrifugal loads resulted in the decision to build the technology demonstrator exclusively with an unstiffened EPDM skin. The results showed that it is possible to incorporate CFRP into an EPDM sandwich, but many questions remained unanswered at this stage. In particular, the fiber impregnation in combination with the EPDM material poses a great challenge, with simultaneously high demands on the smoothness and contour fidelity of the skin. Also, the reversibility of the skin is crucial, especially in the case of many altered morphing conditions. Due to the fact that the skin cannot be replaced in the technology demonstrator, it was decided to use a pure EPDM skin to minimize the risk.

5. TECHNOLOGY DEMONSTRATOR

The demonstrator consists of a combination of different materials. The aluminum spar is the basis for the entire demonstrator. Most of the components could be prefabricated or manufactured from semi-finished products. For example, the GFRP inlays bonded to the aluminum spar were cut from sheet material and then milled to contour. The same applies to the CFRP trailing edge and the GFRP webs, which form the support structure for the elastic skin (Figure 12).

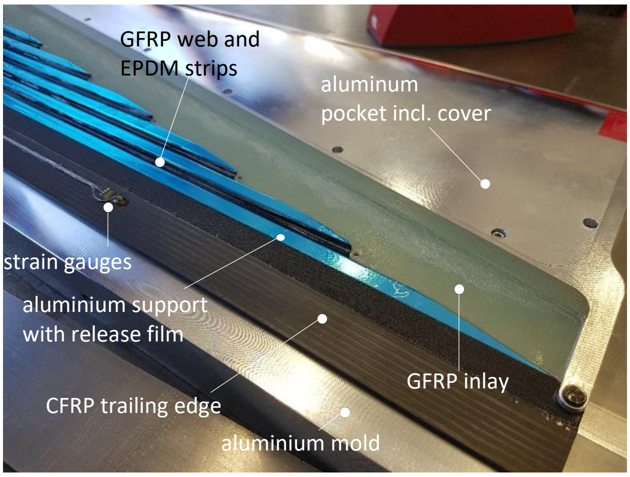

Figure 12: Assembly of technology demonstrator before applying EPDM skin

All these components were instrumented with strain gauges prior to any further steps. The EPDM contact surfaces of the leading and trailing edges are subsequently treated with resin and a tear-off fabric to create a defined, rough surface and improve the adhesion of the elastic skin. The fittings of the webs are glued as a separate assembly and represent the link between the aluminum spar and the fixing rail (Figure 13). The webs can thus move with the respective morphing condition and thus ensure the contour accuracy of the profile.

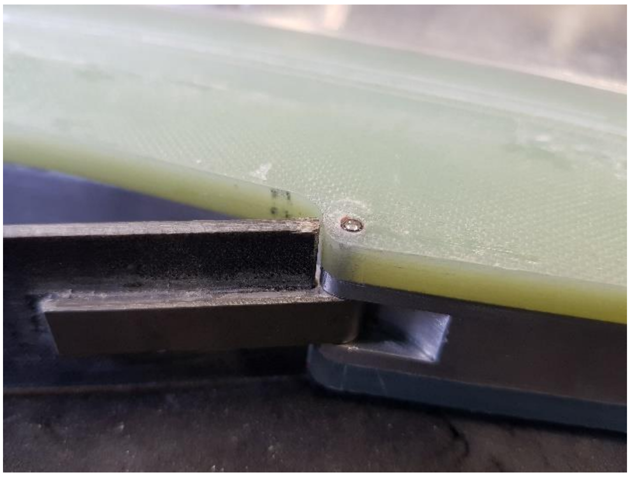
Figure 13: Fitting of the webs

In a final step, the elastic skin, is bonded to the preassembled demonstrator. Since the EPDM temporarily loses viscosity in the vulcanization process step, additional tools are required to close the space between the webs and prevent the elastic material from spreading. These tools are made of aluminum and wrapped with a release film so that the tools can be removed in a later process step. The contact area of the elastic skin to the webs can be increased by means of recesses filled with EPDM strips (Figure 14) on the tools.

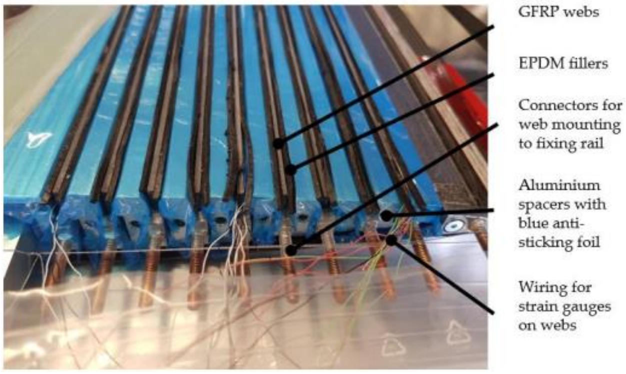

Figure 14:Assembly of technology demonstrator before applying EPDM skin (blade root)

After the demonstrator has been placed in the lower aluminum mold above the lower EPDM skin and the webs and also the spacers have been mounted, the last step is to place the upper EPDM skin (Figure 15). This is fixed with the aid of a cover plate and the entire assembly is then packed as a vacuum setup.


Figure 15:Assembly of technology demonstrator with applied EPDM skin (blade root)

After the autoclave process, the tools between the webs have to be removed again (Figure 16). Preliminary tests have already shown that an additional separating layer is required between the tools and the elastic EPDM skin in order to overcome the adhesive bond between the two components during removal. For this purpose, the tools are wrapped in a blue release film, which is removed after removal of the tool. In addition, compressed air as a release agent has a positive effect on tool disassembly.

Figure 16: Removing aluminum tools with anti sticking foil

Due to a problem during the final production step, the elastic skin has partially fallen below the nominal dimension of 1.6 mm in the root area. This results in gaps, as shown in Figure 16. Towards the tip of the blade, the skin thickness increases again. As a consequence, the skin was cut 60 mm radially from the root edge along the chord direction to avoid further tearing of the skin in radial direction. Furthermore, due to the manufacturing process, the threaded bolts of the two rear webs are missing so that they cannot be guided through the fixing rail. As a further consequence, the blade chord extension of the demonstrator was limited to 30% during the tests.

The surface of the EPDM skin is quite smooth after final assembly. Only a few minor irregularities due to pores or air bubbles are visible. As expected, however, isolated webs are clearly visible in the skin surface (Figure 17). By increasing morphing, the skin is correspondingly stretched. Since there is no other support structure, the skin narrows slightly between two webs and does not follow the desired profile exactly.

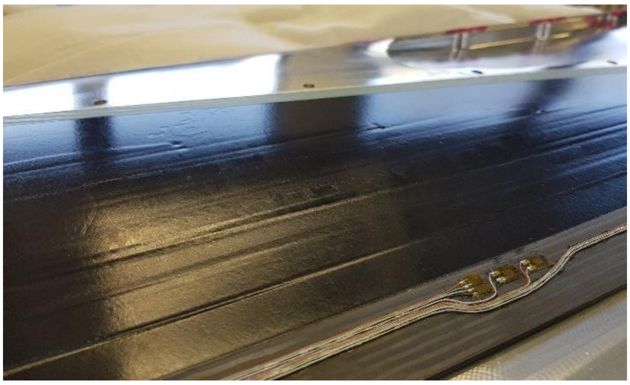

Figure 17: skin condition after assembly

In a final step, the missing pocket cover of the spar is closed with a 3D-printed variant and demonstrator is provided with the remaining stiffening elements. All strain gauges are still brought out at the blade root and prepared for connection to the measuring system before the demonstrator is finally installed in the test stand of the DLR whirl tower in Braunschweig (Figure 18).

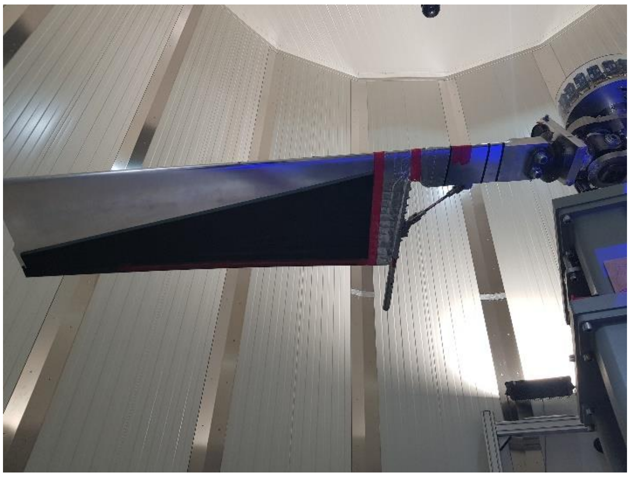

Figure 18: Complete technology demonstrator installed in the whirl tower

Figure 19: optical outer surface investigation of demonstrator with 30% chord extension

One aspect of the experimental phase was to check the accuracy of the outer contour between the demonstrator and the FE simulation for different morphing states. The ATOS system was used for this purpose (Figure 19). This is an optical 3D scanner based on fringe projection that provides traceable 3D coordinates.

Of interest is for example the relative difference in height between the areas bounded by two webs and the adjacent webs themselves. These are relatively close: 0.75 mm between the first and second webs and 0.58 mm between the fourth and fifth webs. From this, it can be deduced that the real out-of-plane deformation in the thickness direction of the profile is greater than originally assumed. The reason for this may be the accumulation of material in the area of the webs, which are supposed to form a better connection, and the associated increased stiffness. This increases the absolute elongation between the webs and the resulting buckling. For a detailed representation, Figure 20 shows a cross section. Note an offset of 1 mm in the simulation data (red pluses) for better clarity. This illustrates the differences and similarities between simulation and measurement already described. More detailed results of the surface analysis are shown in [8].

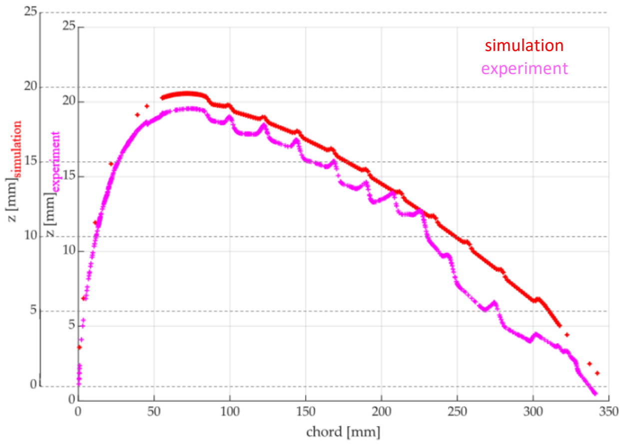

Figure 20: Comparison of the surfaces of Atos measurement (pink plus) and simulation (red pluses) in a sectional view with unequal axes. Values of the simulation have an offset of 1 mm for better

6. CONCLUSIONS

In summary, the following findings could be presented:

- the chosen KRAIBURG EPDM is suitable for the production of elastic skins with very high elastic deformations
- A manufacturing strategy was presented, which enables the adhesion to spar, webs, and trailing edge with different materials in a single process. This successful process is a milestone for the manufacturing of flexible skins and the implementation of the needed supports.
- However, it was also shown that the handling of EPDM is not trivial and the implementation of fibers to stiffen the skin is a major challenge.
- By implementing the actuation concept and bonding the flexible EPDM skin, surface quality and maintaining contour accuracy are most important points to consider

ACKNOWLEDGMENT

This work was funded by the European Research Council (ERC) under the European Union’s Horizon 2020 research and innovation programme, as part of the Shape Adaptive Blades for Rotorcraft Efficiency (SABRE) programme (grant agreement No 723491).

REFERENCES

[1] Ameduri, S., Concilio, A., Galasso, B.: *Modeling and design of an experimental demonstrator of blade twist through the SMA technology*, SMASIS 2019, September 2019.

[2] Barbarino, S., Gandhi, F., Webster,S.D.: *Design of extendable chord sections for morphing helicopter rotor blades*, Journal of Intelligent Material Systems and Structures, 22(9):891–905, 2011.

[3] Moser, P., Barbarino, S., Gandhi, F.: *Helicopter rotor blade chord extension morphing using a centrifugally actuated von mises truss*, Journal of Aircraft, 51(5):1422–1431, 2014.

[4] Gandhi, F., Hayden,E.: *Design, development, and hover testing of a helicopter rotor blade chord extension morphing system*, Smart Materials and Structures, 24, 03 2015.

[5] Riemenschneider, J., Balzarek, C.G., van der Wall, B.G., Majeti, R.K.: *Chord morphing for helicopter rotor blades*, SMASIS 2019, 09.-11.09.2019, Louisville, Kentucky , USA.

[6] Balzarek, C.; Riemenschneider, J.; Majeti, R.K.: Concept of a variable chord-extension, 46th European Rotorcraft Forum, Moscow, Russia, 8–11 September 2020; p. 113

[7] Majeti, R.K.; van der Wall, B.G.; Balzarek, C.G. *Linearly variable chord-extension morphing for helicopter rotor blades*, CEAS Aeronaut. J. 2020, 12, 55–67.

[8] Balzarek, Christoph und Kalow, Steffen und Riemenschneider, Johannes und Rivero, Andres (2022) *Manufacturing and testing of a variable chord extension for helicopter rotor blades,* Actuators, Multidisciplinary Digital Publishing Institute (MDPI). ISSN 2076-0825.